

# The ratio of the beauty structure functions $R^b = \frac{F_L^b}{F_2^b}$ at low- $x$

G.R.Boroun\*

*Physics Department, Razi University, Kermanshah 67149, Iran*  
(Dated: June 3, 2014)

We study the structure functions  $F_k^b(x, Q^2)$  ( $k = 2, L$ ) and the reduced cross section  $\sigma_r^b(x, Q^2)$  for small values of Bjorken's  $x$  variable with respect to the hard (Lipatov) pomeron for the gluon distribution and provide a compact formula for the ratio  $R^b$  that is useful to extract the beauty structure function from the beauty reduced cross section, in particular at DESY HERA. Also we show that the effects of the nonlinear corrections to the gluon distribution tame the behavior of the beauty structure function and the beauty reduced cross section at low  $x$ .

## 1. INTRODUCTION

The measurement of the inclusive beauty quark (b-quark) cross section and the derived structure function  $F_2^{b\bar{b}}$  in DIS at HERA is an important test of the theory of the strong interaction, quantum chromodynamics (QCD), within the Standard Model. Precise knowledge of the parton density functions (PDFs) is for example essential at the Large Hadron Collider (LHC). The b-quark density is important in Higgs production at the LHC in both the Standard Model and in extensions to the Standard Model such as supersymmetric models at high values of the mixing parameter  $\tan\beta$  [1]. First measurements [2] of the b-quark cross sections at HERA were significantly higher than the QCD predictions calculated at next-to-leading order (NLO) approximation. The theoretical NLO QCD predictions are more than three standard deviations below the experimental data. At the Tevatron, old analyses indicated that the overall description of the data can be improved [3] by adopting the non-perturbative fragmentation function of the b-quark into the B-meson: an appropriate treatment of the b-quark fragmentation properties considerably reduces the disagreement between measured beauty cross section and the results of corresponding NLO QCD calculations. Also the latest measurement [4] of beauty photo-production at HERA is in a reasonable agreement with the NLO QCD predictions or somewhat higher. This measurement of the beauty contribution to the inclusive proton structure function  $F_2(x, Q^2)$  have been presented for small values of the Bjorken scaling variable  $x$ , namely  $1E-4 < x < 6E-2$ , and for moderate and high values of the photon virtuality  $Q^2$ , namely  $5 \leq Q^2 \leq 2000 \text{ GeV}^2$ . These data were based on a dataset with an integrated luminosity of  $189 \text{ pb}^{-1}$ , which was about three times greater than in the previous measurements. The data was recorded in the years 2006 and 2007 with  $54 \text{ pb}^{-1}$  taken in e-p mode and  $135 \text{ pb}^{-1}$  in  $e^+p$  mode. The e-p

center of mass energy is  $\sqrt{s} = 319 \text{ GeV}$ , with a proton beam energy of  $E_p = 920 \text{ GeV}$  and electron beam energy of  $E_e = 27.6 \text{ GeV}$  [4].

In the one-photon exchange approximation, beauty meson production in deeply inelastic  $ep$  scattering is via the photon-gluon fusion subprocess  $\gamma^* + g \rightarrow b + \bar{b}$  and therefore sensitive to the gluon density in a proton  $f_g(x, \mu^2)$ . The beauty structure function  $F_2^{b\bar{b}}$  is obtained from the measured beauty-meson cross section after applying small correction for the longitudinal structure function  $F_L^{b\bar{b}}$  [5]. In the framework of DGLAP dynamics [6], the leading contribution to the beauty meson production is given by two basic methods. One of them is based on the massless evolution of parton distributions and the other one is based on the massive boson-gluon fusion matrix element convoluted with the gluon density of the proton [7-17]. The reduced cross section for beauty quark introduced by H1 Collaboration

$$\begin{aligned} \sigma_r^{b\bar{b}} &= \frac{Q^4 x}{2\pi\alpha^2 Y_+} \frac{d^2 \sigma^{b\bar{b}}}{dx dy} \\ &= F_2^{b\bar{b}}(x, Q^2, m^2) - \frac{y^2}{Y_+} F_L^{b\bar{b}}(x, Q^2, m^2) \\ &= F_2^{b\bar{b}}(x, Q^2, m^2) \left(1 - \frac{y^2}{Y_+} R^b\right), \end{aligned} \quad (1)$$

where in earlier HERA analysis,  $F_L^{b\bar{b}}$  was taken to be zero for simplicity. But for the NLO analysis the  $F_L^{b\bar{b}}$  contribution was subtracted from data. Therefore determination of the longitudinal beauty structure function at low  $x$  at HERA is important because the  $F_L^{b\bar{b}}$  contribution to the beauty cross section can be sizeable. Here, we use the hard (Lipatov)Pomeron behavior of structure functions and determine the ratio of the beauty structure functions  $R^b = \frac{F_L^{b\bar{b}}}{F_2^{b\bar{b}}}$  from this behavior in the limit of low  $x$ . The low- $x$  asymptotic behavior of the parton densities are given by

$$f(x, Q^2)|_{x \rightarrow 0} \rightarrow 1/x^{1+\delta}, \quad (2)$$

where  $\delta$  is corresponding to the hard (Lipatov) Pomeron intercept [18-20]. In the low- $x$  range, the gluon and

---

\*Electronic address: grboroun@gmail.com; boroun@razi.ac.ir

quark-singlet contributions are matter while the non-singlet contributions are small. However, our analysis shows that the predictions for  $R^b$  with hard Pomeron intercept describe the inclusive structure function with good accuracy to NLO at low- $x$ , and this analysis is independent of the DGLAP evolution of the gluon distribution function.

In the present letter we use the hard-Pomeron method to derive the ratio of the beauty structure function and the reduced beauty cross section in the region  $Q^2 > m^2$  at low- $x$ . Section 2 is devoted to the numerical solution of the master equation for the beauty structure functions using gluon distribution parameterizations. Then we consider the nonlinear corrections to the gluon distribution function with respect to the GLR-MQ equation for the  $F_2^b(x, Q^2)$  and  $\sigma_r^b(x, Q^2)$ . Our results and conclusions are given in sect.3.

## 2. THE METHOD

In the twist-2 approximation, for the beauty flavor case, the beauty structure functions  $F_i^{b\bar{b}}(x, Q^2)$ , ( $i = 2, L$ ) are described by

$$F_i^b(x, Q^2; m_b^2) = \sum_j C_i^j(a_s, x, \frac{Q^2}{\mu^2}) \otimes f_j(x, \mu^2), \quad (3)$$

where  $a_s = \frac{\alpha_s(\mu^2)}{4\pi}$ ,  $f_j(x, \mu^2)$  are the parton densities and  $C_i^j(a_s, x, \frac{Q^2}{\mu^2})$  are the coefficients functions. Here the mass factorization scale  $\mu$  is assumed to be either  $\mu^2 = 4m_b^2$  or  $\mu^2 = 4m_b^2 + Q^2$ , and the symbol  $\otimes$  for heavy flavour structure functions denotes convolution according to the integral

$$[A \otimes B](x) = \int_{\zeta}^1 \frac{dz}{z} A(z) B(\frac{x}{z}), \quad (4)$$

where  $\zeta = x(1 + 4\xi)$  ( $\xi \equiv \frac{m_b^2}{Q^2}$ ). In the  $\overline{MS}$  scheme, the coefficient functions  $C_i^j$  depend on the scaling variables  $\eta (= (s - 4m_b^2)/4m_b^2)$  and  $\xi$ , where  $s$  is the square of the center of mass energy of the virtual photon-parton subprocess  $Q^2(1 - z)/z$  and  $z$  is the fraction of energy carrying by the parton as

$$z = \frac{Q^2}{2q \cdot p_p},$$

where  $p_p$  is the partonic four-momentum transfer in boson-parton fusion processes. Based on the hard-Pomeron behavior for the parton densities at low- $x$  (Eq.2), we determine the solutions of the beauty structure functions in Eq.3. After the conventional integration (according to Eq.4) and doing some rearranging, Eq.3 can

be rewritten as

$$F_i^b(x, Q^2; m_b^2) = \sum_{j=g,S} x f_j(x, \mu^2) [C_i^j(a_s, x, \frac{Q^2}{\mu^2}) \otimes z^\delta], \quad (5)$$

with hard behavior for the intercept at Regge factorization, where  $[...] = \int_x^{\frac{1}{x}} C_i^j(., z) z^\delta dz$  and  $a = 1 + 4\xi$ . Thus, considering structure functions with respect to hard intercept are given by the following expression

$$F_i^b(x, Q^2; m_b^2) = x f_g(x, \mu^2) [C_i^g(a_s, x, \frac{Q^2}{\mu^2}) \otimes z^\delta] + x f_S(x, \mu^2) [C_i^S(a_s, x, \frac{Q^2}{\mu^2}) \otimes z^\delta]. \quad (6)$$

Here the coefficient functions are defined with respect to their origin. The coefficient function  $C^g$  originate from the partonic subprocesses where the virtual photon is coupled to the heavy quark, whereas the  $C^S$  comes from the subprocess where the virtual photon interacts with the light quark. The lowest order term contains only the gluon density so that its proportional to  $C^g$ . Whereas the light quark densities only come in next order analysis and those is about 5%. Then  $F_i^b$ 's are used in global analyses constrain the gluon density. Besides the gluon density, the main source of theoretical uncertainty in  $F_i^b$ 's is the values of the beauty renormalization scales. Therefore, a further simplification is obtained by neglecting the  $\gamma^* q(\bar{q})$  fusion subprocesses in Eq.6, which is justified because their contributions vanish at LO and are small at NLO for small values of  $x$  [21]. Thus, we derive the low- $x$  approximation formula for the beauty structure functions at LO up to NLO by the following form

$$F_i^b(x, Q^2; m_b^2) \simeq x f_g(x, \mu^2) [C_i^g(a_s, x, \frac{Q^2}{\mu^2}) \otimes z^\delta]. \quad (7)$$

Our prediction for the ratio of the beauty structure functions  $R^b$  is independent of the gluon density at low- $x$ , as

$$R^b = \frac{F_L^b}{F_2^b} = \frac{[C_L^g(a_s, x, \frac{Q^2}{\mu^2}) \otimes z^\delta]}{[C_2^g(a_s, x, \frac{Q^2}{\mu^2}) \otimes z^\delta]}. \quad (8)$$

In the above expression  $C_j^g$ 's are the gluonic coefficient functions expressed in terms of LO and NLO contributions in beauty-quark leptonproduction as follows

$$C_j^g \rightarrow C_{j,g}^0 + a_s(\mu^2) [C_{j,g}^1 + \bar{C}_{j,g}^1 \ln \frac{\mu^2}{m_b^2}]. \quad (9)$$

The coefficients  $C_{j,g}^0$  and  $C_{j,g}^1$  ( $\bar{C}_{j,g}^1$ ) are at LO and NLO respectively. These coefficient functions have been computed at LO up to NLO in Refs. [7-9,22-27]. We conclude that the ratio of the beauty structure functions

(the Callan-Gross ratio) in heavy-quark leptonproduction is a phenomenological observable quantitatively defined in pQCD. With respect to the experimental aspect, it is useful for extraction of the reduced beauty cross section from the phenomenological relation for structure function  $F_2^b$  and the ratio  $R^b$  as follows

$$\sigma_r^{b\bar{b}} = x f_g(x, \mu^2) [C_2^g(a_s, x, \frac{Q^2}{\mu^2}) \otimes z^\delta] \times (1 - \frac{y^2 [C_L^g(a_s, x, \frac{Q^2}{\mu^2}) \otimes z^\delta]}{Y_+ [C_2^g(a_s, x, \frac{Q^2}{\mu^2}) \otimes z^\delta]}). \quad (10)$$

This formula can reproduce the HERA results for the beauty reduced cross section from the phenomenological models for the gluon distribution function at low- $x$ .

At low- $x$ , the high-density gluon distributions are singular for  $b\bar{b}$  meson production. The density of low momentum-fraction gluons is expected to be close to saturation of the available phase space, so as to produce significant recombination effects. Therefore, the gluon distribution function will be close to phase-space saturation and here will be important gluon-fusion effects ( $gg \rightarrow g$ ). These effects can be accounted for the gluon scale evolution equation by adding a negative nonlinear (quadratic) term to the standard linear DGLAP term as

$$\frac{\partial f_g(x, Q^2)}{\partial \log Q^2} = [\text{DGLAP term of order}(f_g)] - [\text{term of order}(f_g^2)]. \quad (11)$$

Therefore, the linear evolution equation in this case is modified by non-linear term description gluon recombination. An important point in the gluon saturation approach is the  $x$ -dependent saturation scale  $Q_s^2(x)$ . This scaling argument leads to the conclusion that  $\gamma^*p$  cross section, which is *a priori* function of two independent variable ( $x$  and  $Q^2$ ), is a function of only variable  $\tau = \frac{Q^2}{Q_s^2(x)}$ . In the limit of high energy, PQCD consistently predicts that the high gluon density should form a Color Glass Condensate (CGC), where the interaction probability in DIS becomes large and this is characterized by a hard saturation scale  $Q_s(x)$  which grows rapidly with  $1/x$  [28-37]. In this region, the nonlinear saturation dynamics is incorporated into the CGC model. As, it is valid only for  $Q^2$  less than or of the order of the saturation momentum, which is at most several  $GeV^2$ , while the fit result to SGK [31] model extends up to  $Q^2$  of the order of several hundred  $GeV^2$ . The overall physical picture is dependence to the different regions in the  $(x, Q^2)$ -plane. For  $Q^2 < Q_s^2(x)$  the linear evolution is strongly perturbed by nonlinear effects where the parton system becomes dense and the saturation corrections start to play an important role. In color-dipole (CD) model the excitation of heavy flavors at low- $x$  is described in terms of interaction of small size quark-antiquark  $b\bar{b}$

color dipoles in the photon. This interaction can be defined by the  $\Psi_{L,T}^{b\bar{b}}(z, r)$ , where it is the probability to find the  $b\bar{b}$  color dipole in the photon with respect to the  $\sigma^{b\bar{b}}(x, Q^2)$ . Here  $z$  is the carrying fraction by the beauty quark into the photons light-cone momentum and  $r$  is the size of the  $b\bar{b}$  interaction in the photon. In this region the dipole cross section is bounded by an energy independent value, as the dipole cross section was proposed [28-37] to have the form  $\sigma_{dipole}(x, r) = \sigma_0 \{1 - \exp(-r^2 Q_s^2(x)/4)\}$  which impose the unitarity condition ( $\sigma_{q\bar{q}} \leq \sigma_0$ ) for large dipole sizes  $r$ . The CD cross section is given by color dipole factorization formula

$$\sigma^{b\bar{b}}(x, Q^2) = \int_0^1 \int d^2\mathbf{r} [|\Psi_L^{b\bar{b}}(z, \mathbf{r})|^2 + |\Psi_T^{b\bar{b}}(z, \mathbf{r})|^2] \times \sigma_{dipole}(x, \mathbf{r}). \quad (12)$$

At small - $r$  region, the dipole cross section is related to the gluon density where it is valid in the double logarithmic approximation. As the gluon density is  $xg(x, Q^2 = Q_s^2(x)) = r_0 x^{-\lambda}$ , and the parameter  $r_0$  specifies the normalization along the critical line. Thus, the saturation scale is an intrinsic characteristic of a dense gluon system. At low- $x$  region, the CD cross section satisfies the solutions with Regge behavior for the beauty structure function of the proton as

$$F_2^b(x, Q^2) = \frac{Q^2}{4\pi^2 \alpha_{em}} \sigma^{b\bar{b}}(x, Q^2) = \sum_n f_n^b(Q^2) (\frac{x_0}{x})^{\Delta_n} \quad (13)$$

where  $n = soft, 0, 1, ..$  and the choice  $x_0 = 0.03$  [9-10,12]. The intercepts  $\Delta_n$  are equal to  $\Delta_0/(1+n)$ , where  $\Delta_0$  is defined with respect to the hard Lipatov pomeron and the coefficients  $f_n^b(Q^2)$  are presented in Ref.12 (V.R.Zoller, Phys.Lett. **B509**, 69(2001)). The observation of the QCD pomeron dynamics at distances  $\sim m_b^{-1}$  leads to exchange beauty exponent from  $\Delta_n$  to  $\Delta_{eff}$ , where  $\Delta_{eff}$  is defined by

$$\Delta_{eff} = \Delta_0 [1 - \sum_{n=1} r_n (1 - \frac{\Delta_n}{\Delta_0}) (\frac{x_0}{x})^{\Delta_n - \Delta_0}]. \quad (14)$$

At what follows, we consider Eq.11 for the behavior of the beauty structure functions as the recombination processes between gluons in a dense system have to be taken into account and it has to be tamed by screening effects. These nonlinear terms reduce the growth of the gluon distribution in this kinematic region where  $\alpha_s$  is still small but the density of partons becomes so large. Gribov, Levin, Ryskin, Mueller and Qiu (GLR-MQ) [38-39] argued that the physical processes of interaction and recombination of partons become important in the parton cascade at a large value of the parton density, and that these shadowing corrections could be expressed in a new evolution equation (the GLRMQ equation).

Therefore, the evolution equations of gluons can be modified as

$$\frac{\partial x f_g(x, Q^2)}{\partial \ln Q^2} = \frac{\partial x f_g(x, Q^2)}{\partial \ln Q^2} \Big|_{DGLAP} - \frac{\alpha_s^2 \gamma}{R^2 Q^2} \int_{\chi}^1 \frac{dy}{y} [y f_g(y, Q^2)]^2, \quad (15)$$

where the first term is the linear standard DGLAP evolution and the second term is defined with respect to the 2-gluon density [40-41]. In this equation,  $\gamma$  is equal to  $\frac{81}{16}$  for  $N_c = 3$  and  $R$  is the size of the target which the gluons populate becomes so large that the annihilation of gluons becomes important.  $R$  will be of the order of the proton radius ( $R \simeq 5 \text{ GeV}^{-1}$ ) if the gluons are spread throughout the entire nucleon, or much smaller ( $R \simeq 2 \text{ GeV}^{-1}$ ) if gluons are concentrated in hot-spot [42] within the proton. Here  $\chi = \frac{x}{x_0}$  where  $x_0 (= 0.01)$  is the boundary condition that the gluon distribution joints smoothly onto the unshadowed region. In this equation we need to determine the appropriate behavior of the shadowing corrections to the gluon distribution at the initial point. Where the unshadowed distribution to the gluon ( $f_g^u$ ) at  $Q_0^2$  has to modify for  $x < x_0$  as

$$x f_g(x, Q_0^2) = x f_g^u(x, Q_0^2) [1 + \theta(x_0 - x) [x f_g^u(x, Q_0^2) - x f_g^u(x_0, Q_0^2)] / x f_g^{sat}(x, Q_0^2)]^{-1}, \quad (16)$$

here  $x f_g^{sat}(x, Q^2) = \frac{16 R^2 Q^2}{27 \pi \alpha_s(Q^2)}$  is the value of the gluon which would saturate the unitarity limit in the leading shadowing approximation. Equation (16) reduces to the unshadowed form  $x f_g^u$  when shadowing is negligible; that is, when  $x f_g^{sat} \rightarrow \infty$ . In this region, the interaction of gluons is negligible and we use the linear evolution equations in  $x f_g(x, Q^2)$ . However, at sufficiently low- $x$ , two gluons in different cascades may interact and so decrease the gluon density. Therefore, we apply the saturation corrections to the gluon distribution function in Eqs.7 and 10 to obtain the shadowing corrections for the beauty structure function and the beauty reduced cross section behavior and show that this behavior tame at low- $x$  limit.

### 3. RESULTS AND CONCLUSIONS

In this work, the beauty structure functions, the ratio of the beauty structure functions and the reduced beauty cross sections at  $Q^2 = 60$  and  $650 \text{ GeV}^2$  have determined. We compared our results with H1 data on beauty production [4], color dipole model [9-10,12] and the GJR parametrisation [43]. In Figs.1 and 2 the beauty structure functions and reduced cross section with respect to the gluon distribution function at the renormalization scale  $\mu^2 = 4m_b^2 + Q^2$  with  $m_b = 4.57 \text{ GeV}$  are

shown. We observe that these relations (Eqs. 7 and 10) are dependence to the gluon distribution, which is usually taken from the GRV [22] and Block [44] parameterizations or DL [18-20] model. In what follows we shall use the gluon distribution with an intercept according to the hard pomeron behavior at the DL model. These results show that the fractional accuracy for the DL model with a hard pomeron intercept is the best which confirms the correctness of our solution with DL model when compared with H1 data, color dipole model and GJR parametrisation. For comparing with H1 data (2010) [4], we presented our results from  $Q^2 = 5 \text{ GeV}^2$  up to  $2000 \text{ GeV}^2$  in Table 1. The theoretical uncertainties in our result are according to the renormalization scales  $\mu^2 = 4m_b^2 + Q^2$  and  $\mu^2 = 4m_b^2$ . We observe that the theoretical uncertainties, for the beauty functions, related to the freedom in the choice of  $\mu$  are negligibly small. The agreement between our predictions with the results obtained by H1 Collaboration is remarkably good at the renormalization scale  $\mu^2 = 4m_b^2 + Q^2$  and with the DL parton distribution function. As can be seen in all figures, the increase of our calculations for the beauty structure functions towards low  $x$  are consistent with the experimental data.

In Fig.3 we show the predicted ratio of the beauty structure functions,  $R^b$ , as a function  $Q^2$  at  $x = 0.001$ . This ratio is independent of the choice of the gluon distribution function, where approaches based on perturbative QCD and  $k_T$  factorization give similar predictions [13-15]. The  $R^b$  effect on the corresponding differential beauty cross section should be considered in extraction of  $F_2^b$ . We see that this value is approximately between 0.10 and 0.20 in a region of  $Q^2$  and this prediction for  $R^b$  is close to the results Refs. [13-15]. We can see that the behavior of this ratio is in agreement with the prediction from Ref.[8]. As authors obtained an approximate formula at LO and NLO analysis for low- $x$  values, where at LO the compact form is

$$R^b \approx \frac{2}{1 + 4\xi} \frac{1 + 6\xi - 4\xi(1 + 3\xi)J(\xi)}{1 + 2(1 - \xi)J(\xi)}, \quad (17)$$

where  $J(\xi) = -\frac{1}{\sqrt{a}} \ln(\frac{\sqrt{a}-1}{\sqrt{a}+1})$ . We compare our result with this compact formula in Fig.3.

In Figs. 4 and 5, the values of the nonlinear corrections to the gluon distribution function determined for predictions of the beauty structure functions and beauty reduced cross section. In Fig.4, we show shadowing corrections to the gluon distribution function determined from Eq.(16) as a function of  $x$  at the initial scale  $Q_0^2 = 5 \text{ GeV}^2$  for determination of the beauty structure function and beauty reduced cross section. In Fig.5, we show the shadowing corrections to the gluon distribution function determined from Eq.(15) at  $Q^2 = 60 \text{ GeV}^2$ . We observed that, as  $x$  decreases, the singularity behavior of the gluon functions are tamed by

shadowing effects. Therefore the singularity behavior of the beauty structure function and beauty reduced cross section are tamed by shadowing effects. The solid curves show the low- $x$  behavior when shadowing is neglected, and the lower curves (dash and dot) show the effect of the shadowing contribution for  $R = 5$  and  $2 \text{ GeV}^{-1}$ , respectively. We compared our results with H1 data [4] and CD model [9-10,12] (dash-dot-dot). These results show that beauty structure function and beauty reduced cross section behaviors are tamed with respect to nonlinear terms at the GLR-MQ equation to the gluon density behavior at low  $x$ . These figures show that screening effects are provided by multiple gluon interaction which leads to the nonlinear terms in the DGLAP equation.

In summary, our numerical results for the beauty structure functions and beauty reduced cross section at low  $x$  are obtained by applying the hard (Lipatov) pomeron behavior at all  $Q^2$  values in the NLO analysis.

We derived the ratio  $R^b = \frac{F_L^{b\bar{b}}}{F_2^{b\bar{b}}}$  that is valid through NLO at small values of Bjorken's  $x$  variable, as it is independent of the input gluon distribution function. To confirm the method and results, the calculated values are compared with the H1 data and other models on the beauty structure function, at low- $x$ . Then we studied the effects of adding the nonlinear GLR-MQ corrections to the DGLAP evolution equation, by adding to the beauty structure function and beauty cross section at low- $x$ . The nonlinear effects to the gluon distribution are found to play an increasingly important at  $x < 0.001$ . We observed that, as  $x$  decreases, the singularity behavior of the beauty structure function and beauty reduced cross section are tamed by shadowing effects. We compared our results with the H1 data and with the CD model.

G.R.Boroun thanks Prof.V.R.Zoller for discussions and useful comments.

## REFERENCES

1. D. Dicus, T. Stelzer, Z. Sullivan, and S. Willenbrock, Phys. Rev. D **59**, 094016(1999); C. S. Huang and S. H. Zhu, Phys. Rev. D **60**, 075012(1999); C. Balazs, H. J. He, and C. P. Yuan, Phys. Rev. D **60**, 114001(1999); J. Campbell, R. K. Ellis, F. Maltoni, and S. Willenbrock, Phys. Rev. D **67**, 095002 (2003); F. Maltoni, Z. Sullivan, and S. Willenbrock, Phys. Rev. D **67**, 093005(2003).
2. C. Adloff et al. (H1 Collaboration), Phys. Lett. B **467**, 156 (1999); Erratum: ibid B **518**, 331 (2001).
3. M. Cacciari and P. Nason, Phys. Rev. Lett. **89**, 122003(2002); M. Cacciari, S. Frixione, M.L. Mangano, P. Nason, and G. Ridolfi, JHEP **0407**, 033(2004).
4. F.D. Aaron et al. [H1 Collaboration], Eur.Phys.J.C **65**, 89 (2010); A.Aktas et al. [H1 Collaboration], Eur.Phys.J.C **45**, 23 (2006); Eur.Phys.J.C **40**, 349 (2005).
5. A.V. Lipatov, N.P. Zotov, JHEP **0608**, 043(2006); Phys.Rev.D **73**, 114018(2006).
6. Yu.L.Dokshitzer, Sov.Phys.JETP **46**, 641(1977); G.Altarelli and G.Parisi, Nucl.Phys.B **126**, 298(1977); V.N.Gribov and L.N.Lipatov, Sov.J.Nucl.Phys. **15**, 438(1972).
7. J.Blimlein, A.De Freitas, W.L.van Neerven and S.Klein, Nucl.Phys.B **755**, 272(2006) .
8. A. Y. Illarionov, B. A. Kniehl and A. V. Kotikov, Phys.Lett. B **663**, 66 (2008).
9. N.Nikolaev, J.Speth and V.R.Zoller, Phys.Lett.B **473**, 157(2000).
10. R.Fiore, N.Nikolaev and V.R.Zoller, JETP Lett **90**, 319(2009).
11. I.P.Ivanov and N.Nikolaev, Phys.Rev.D **65**, 054004(2002).
12. N.N.Nikolaev and V.R.Zoller, Phys.Lett. B **509**, 283(2001); Phys.Atom.Nucl. **73**, 672(2010); V.R.Zoller, Phys.Lett. B **509**, 69(2001);
13. A. V. Kotikov, A. V. Lipatov, G. Parente and N. P. Zotov Eur. Phys. J. C **26**, 51(2002).
14. V. P. Goncalves and M. V. T. Machado, Phys. Rev. Lett. **91**, 202002 (2003).
15. N.Ya.Ivanov, Nucl.Phys.B **814**, 142(2009); Eur.Phys.J.C **59**, 647(2009).
16. G.R.Boroun and B.Rezaei, Nucl.Phys.B **857**, 143(2012); EPL, **100**, 41001(2012); JETP, 2012, Vol.115, No.3, 427(2012).
17. S.Catani, Z.Phys.C **75**, 665(1997).
18. A.Donnachie and P.V.Landshoff, Z.Phys.C **61**, 139(1994); Phys.Lett.B **518**, 63(2001); Phys.Lett.B **533**, 277(2002); Phys.Lett.B **470**, 243(1999); Phys.Lett.B **550**, 160(2002).
19. R.D.Ball and P.V.landshoff, J.Phys.G **26**, 672(2000).
20. P.V.landshoff, arXiv:hep-ph/0203084 (2002).

21. E.Laenen, S.Riemersma, J.Smith and W.L. van Neerven, Nucl.Phys.B **392**, 162(1993).
22. M.Gluk, E.Reya and A.Vogt, Z.Phys.C**67**, 433(1995); Eur.Phys.J.C**5**, 461(1998).
23. V.N. Baier et al., Sov. Phys. JETP 23 104 (1966); V.G. Zima, Yad. Fiz. 16 1051 (1972); V.M. Budnev et al., Phys. Rept. 15 181 (1974).
24. E. Witten, Nucl. Phys. B104 445 (1976); J.P. Leveille and T.J. Weiler, Nucl. Phys. B147 147 (1979); V.A. Novikov et al., Nucl. Phys. B136 125 (1978) 125.
25. A.Vogt, arXiv:hep-ph:9601352v2(1996).
26. E.Laenen, S.Riemersma, J.Smith and W.L. van Neerven, Nucl.Phys.B **392**, 162(1993).
27. S. Catani, M. Ciafaloni and F. Hautmann, Preprint CERN-Th.6398/92, in Proceeding of the Workshop on Physics at HERA (Hamburg, 1991), Vol. 2., p. 690; S. Catani and F. Hautmann, Nucl. Phys. B **427**, 475(1994); S. Riemersma, J. Smith and W. L. van Neerven, Phys. Lett. B **347**, 143(1995).
28. K.Golec-Biernat, J.Phys.G **28**, 1057(2002).
29. K.Golec-Biernat, Acta Phys.Pol.B **35**, 3103(2004).
30. K.Golec-Biernat, Acta Phys.Pol.B **33**, 2771(2002).
31. A.M.Stato, K.Golec-Biernat and J.Kwiecinski, Phys.Rev.Lett.**86**, 596(2001).
32. E.Iancu, K.Itakura and S.Munier, Phys.Lett.B **590**, 199(2004).
33. E.Iancu, K.Itakura and S.Munier, Nucl.Phys.A **708**, 327(2002).
34. L. McLerran and R. Venugopalan, Phys.Rev.D**49**, 2233(1994).
35. E. Iancu, A. Leonidov and L. McLerran, Nucl.Phys.A**692**, 583(2001).
36. E. Iancu, A. Leonidov and L. McLerran, Phys.Lett.B**510**, 133(2001).
37. E. Ferreira, E. Iancu, A. Leonidov and L. McLerran, Nucl.Phys.A**703**, 489(2002).
38. A.H.Mueller and J.Qiu, Nucl.Phys.B**268**, 427(1986).
39. L.V.Gribov, E.M.Levin and M.G.Ryskin, Phys.Rep.**100**, 1(1983).
40. E.Laenen and E.Levin, Nucl.Phys.B**451**, 207(1995).
41. K.J.Eskola, et.al., Nucl.Phys.B**660**, 211(2003).
42. E.M.Levin and M.G.Ryskin, Phys.Rep.**189**, 267(1990).
43. M. Gluck, P. Jimenez-Delgado, E. Reya, Eur.Phys.J.C **53**, 355 (2008).
44. M.M.Block et al., Phys.Rev.D **77**, 094003(2008).

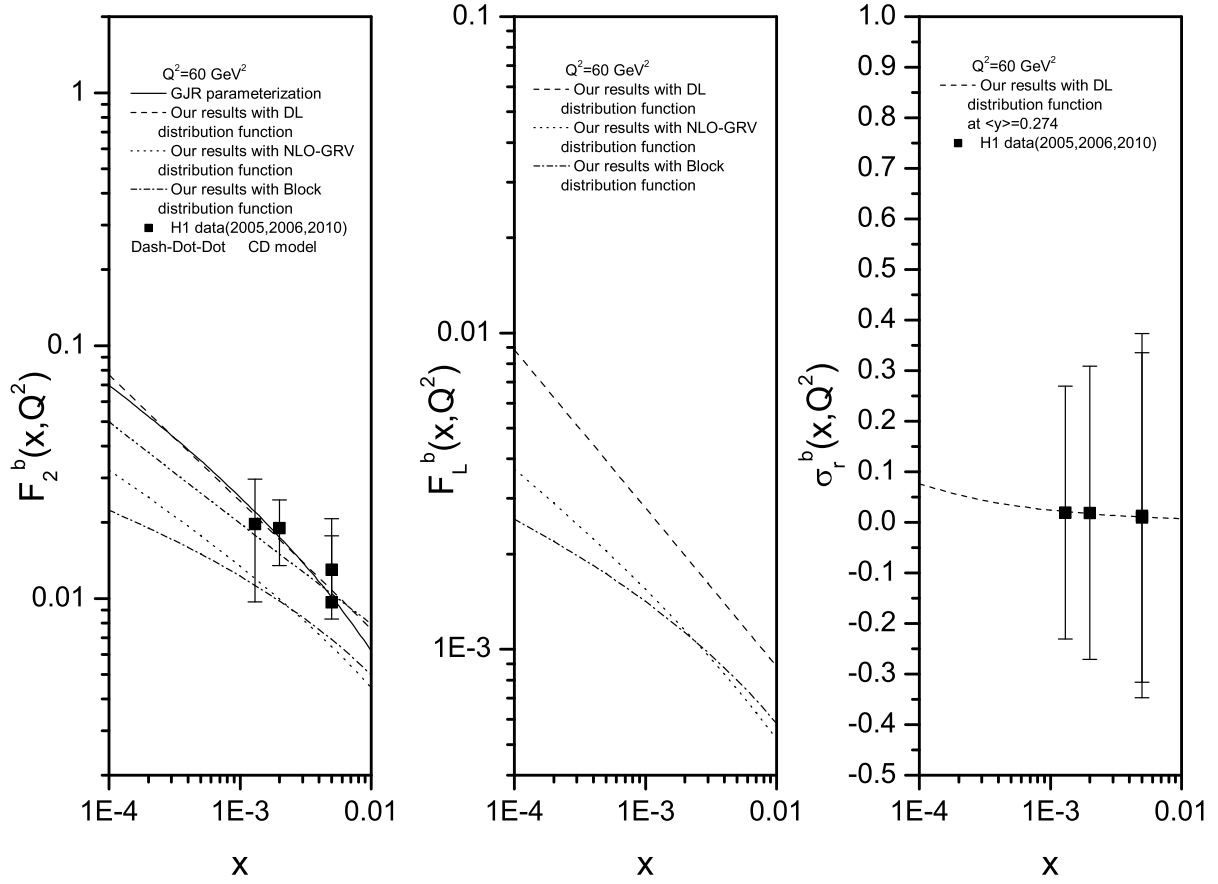


FIG. 1: Predictions for  $F_2^b(x, Q^2)$ ,  $F_L^b(x, Q^2)$  and  $\sigma_r^b(x, Q^2)$  at  $Q^2 = 60 \text{ GeV}^2$  with the input gluon distribution from DL [18-20] model (dash curve), GRV [22] parameterization (dot curve) and Block [44] model (dash-dot curve), compared with color dipole [9-10,12] model (dash-dot-dot curve) and the GJR [43] parameterization (solid curve).

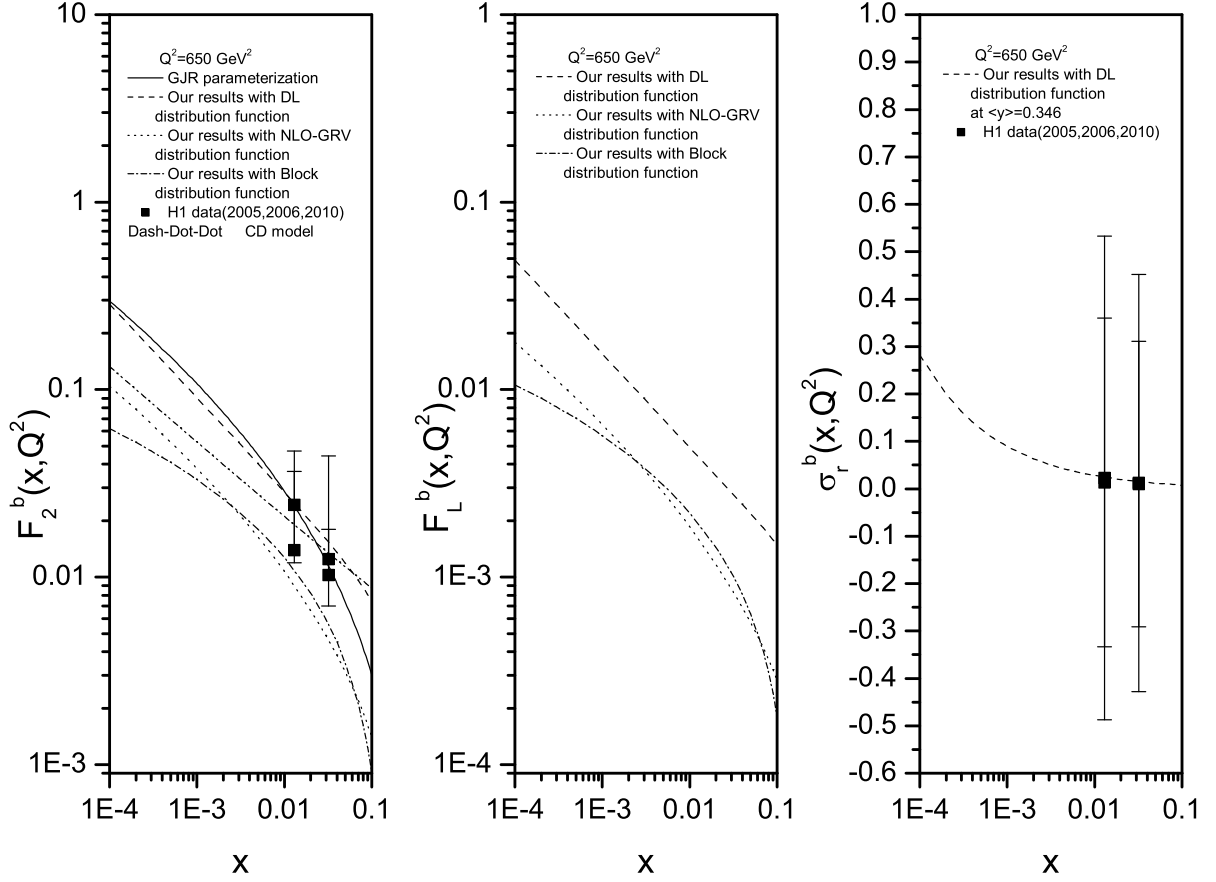


FIG. 2: The same as Fig.1 at  $Q^2 = 650 \text{ GeV}^2$ .

TABLE I: Values of  $F_2^b(x, Q^2)$ ,  $F_L^b(x, Q^2)$  and  $\sigma_r^b(x, Q^2)$  extracted from the DL model at low and high  $Q^2$  (in  $\text{GeV}^2$ ) values at the renormalization scales  $\mu^2 = Q^2 + 4m_b^2$  and  $\mu^2 = 4m_b^2$ , respectively. Also, for comparison, the results determined by H1 Collaboration (2010)[4] are quoted.

$Q^2(\text{GeV}^2)$	$x$	$y$	$\sigma_r^b \text{ (H1 data)} \pm \Delta$	$F_2^b \text{ (H1 data)} \pm \Delta$	$F_2^b$	$F_L^b$	$\sigma_r^b$	$F_2^b$	$F_L^b$	$\sigma_r^b$
5	0.00020	0.246	$0.00244 \pm 0.461$	$0.00244 \pm 0.01$	0.00116	0.186E-4	0.00115	0.00116	0.187E-4	0.00116
12	0.00032	0.369	$0.00487 \pm 0.318$	$0.00490 \pm 0.011$	0.00412	0.00015	0.00411	0.00419	0.00015	0.00418
12	0.00080	0.148	$0.00247 \pm 0.435$	$0.00248 \pm 0.011$	0.00260	0.926E-4	0.00260	0.00264	0.94E-4	0.00264
25	0.00050	0.492	$0.01189 \pm 0.251$	$0.01206 \pm 0.013$	0.01040	0.000674	0.01029	0.01075	0.00070	0.01062
25	0.00130	0.189	$0.00586 \pm 0.341$	$0.00587 \pm 0.010$	0.00645	0.000418	0.00644	0.00666	0.00043	0.00665
60	0.00130	0.454	$0.01928 \pm 0.250$	$0.01969 \pm 0.010$	0.02124	0.002454	0.02085	0.02271	0.00263	0.02229
60	0.00500	0.118	$0.00964 \pm 0.326$	$0.00965 \pm 0.011$	0.01078	0.001250	0.01077	0.01152	0.00134	0.01151
200	0.00500	0.394	$0.02365 \pm 0.232$	$0.02422 \pm 0.029$	0.02488	0.00430	0.02439	0.02891	0.00506	0.02834
200	0.01300	0.151	$0.01139 \pm 0.344$	$0.01142 \pm 0.027$	0.01528	0.00267	0.01525	0.01776	0.00314	0.01772
650	0.01300	0.492	$0.01331 \pm 0.347$	$0.01394 \pm 0.033$	0.02480	0.00430	0.02397	0.03220	0.00580	0.03109
650	0.03200	0.200	$0.01018 \pm 0.301$	$0.01024 \pm 0.034$	0.01536	0.00274	0.01530	0.01996	0.00368	0.01987
2000	0.05000	0.394	$0.00499 \pm 0.611$	$0.00511 \pm 0.043$	0.01740	0.00288	0.01710	0.02530	0.00447	0.02480



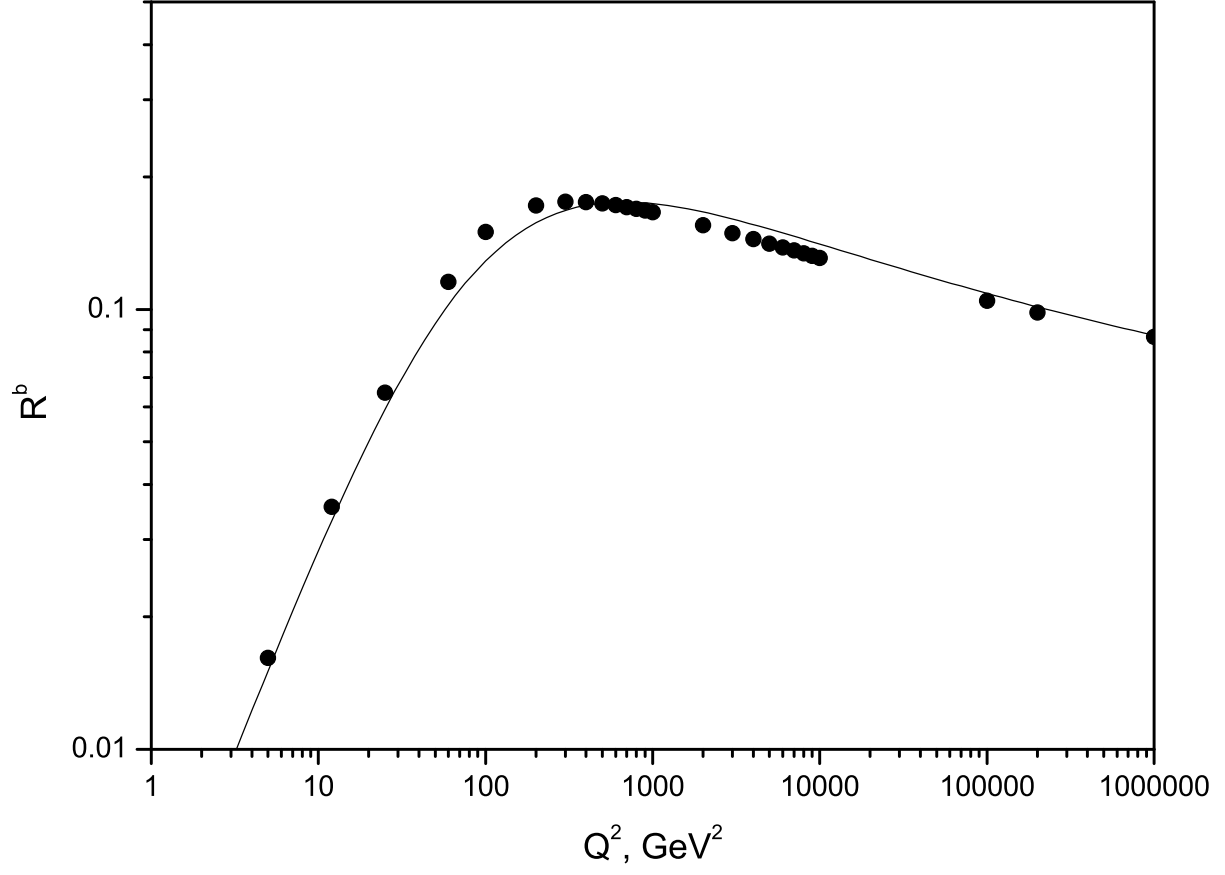


FIG. 3:  $R^b$  evaluated as functions of  $Q^2$  with  $\mu^2 = Q^2 + 4m_b^2$  compared with LO compact formula in Ref.[8](Solid curve).

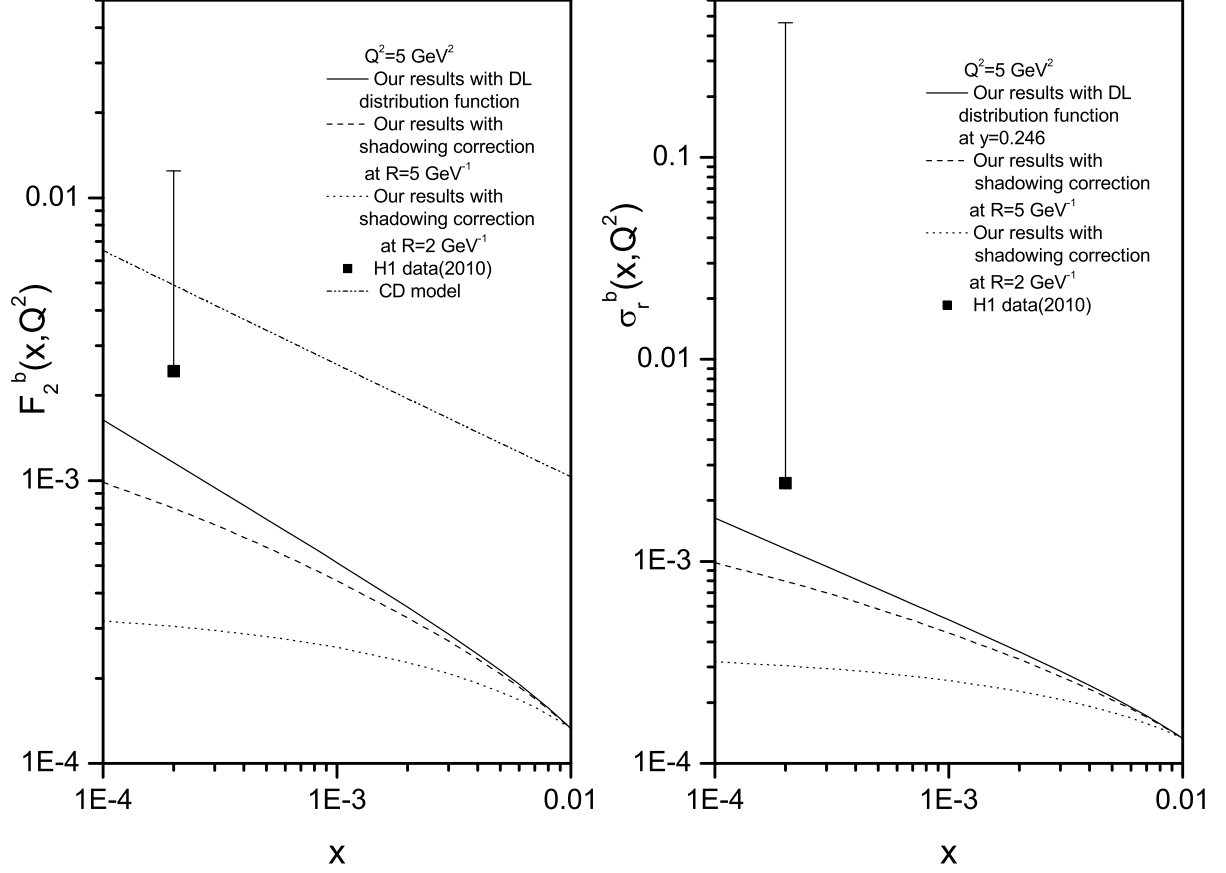


FIG. 4: The shadowing corrections to the  $F_2^b(x, Q^2)$  and  $\sigma_r^b(x, Q^2)$  at  $Q_0^2 = 5 \text{ GeV}^2$  from the solution of the initial condition shadowing effects with the boundary condition at  $x_0 = 0.01$ . The solid curve is the our results with DL model for unshadowed corrections and dash (dot) curves are the shadowing correction included with  $R = 5 \text{ GeV}^{-1}$  ( $= 2 \text{ GeV}^{-1}$ ), respectively, that compared with CD model (dash-dot-dot) and H1 data.

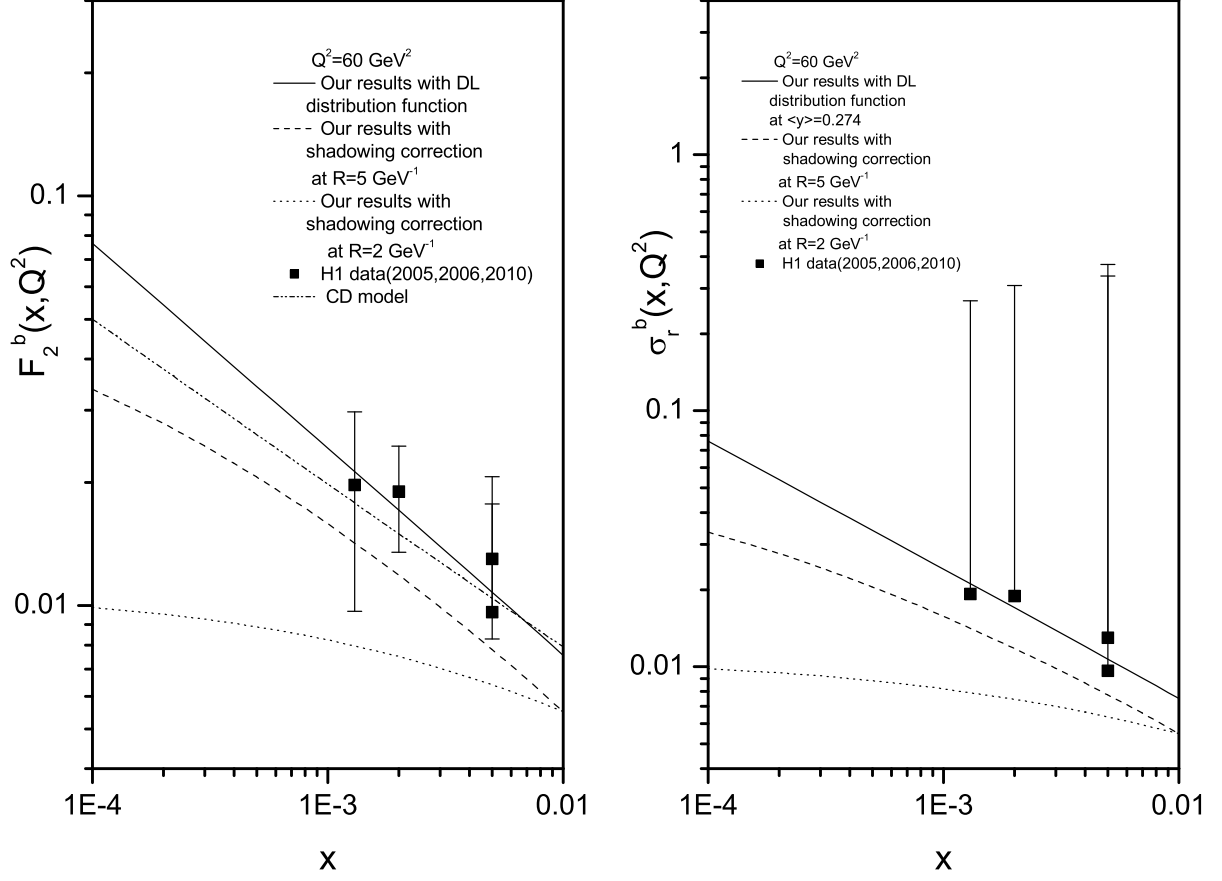


FIG. 5: The same as Fig.4 at  $Q^2 = 60 \text{ GeV}^2$ .